Eulerian–Lagrangian Hybrid Numerical Method for the Longitudinal Dispersion Equation

Jun, Kyung Soo*/Lee, Kil Seong**

ABSTRACT/A hybrid finite difference method for the longitudinal dispersion equation, which is based on combining the Holly–Preissmann scheme with fifth–degree Hermite interpolating polynomial and the generalized Crank–Nicholson scheme, is described and comparatively evaluated with other characteristics–based numerical methods. Longitudinal dispersion of an instantaneously–loaded pollutant source is simulated, and computational results are compared with the exact solution. The present method is free from wiggles regardless of the Courant number, and exactly reproduces the location of the peak concentration. Overall accuracy of the computation increases for smaller value of the weighting factor, θ of the model. Larger values of θ overestimates the peak concentration. Smaller Courant number yields better accuracy, in general, but the sensitivity is very low, especially when the value of θ is small. From comparisons with the hybrid method using cubic interpolating polynomial and with split–operator methods, the present method shows the best performance in reproducing the exact solution as the advection becomes more dominant.

1. Introduction

A number of studies have been carried out on finite difference numerical methods for the longitudinal dispersion equation (Kang and Lee, 1987; Yoon, 1979 ; Abbott and Basco, 1989; Bresler, 1973; Chaudhari, 1971; Leonard, 1979). However, most of the methods do not adequately incorporate the hyperbolicity, or the directionality of the information propagation since they approximate partial derivatives with respect to time and space using fixed computational grid points. Consequently, they often accompany with numerical diffusion or numerical oscillations. Holly and Preissmann (1977) developed an explicit finite difference method, called Holly–Preissmann scheme, for pure advection equation, which takes into account the hyperbolicity of the equation by approximating the total derivative along the characteristic line. Since the characteristic line which passes through a

* Assistant Professor, Dept. of Civil Eng., Sung Kyun Kwan Univ., Suwon, Korea

* * Professor, Dept. of Civil Eng., Seoul National Univ., Seoul, Korea

grid point at current time level does not necessarily come from a grid point of the previous time level, it is needed to express the concentrations at any spatial points in terms of those at fixed Eulerian grid points. To do this they introduced a Hermite interpolating polynomial of the Courant number with coefficients expressed in terms of concentrations and their spatial derivatives at two adjacent grid points. They also extended the method to the advection-diffusion equation by approximating the diffusion term by the second-order partial derivative of the interpolating polynomial.

Holly and Polatera (1984) developed a split-operator method for two-dimensional advective diffusion equation. They decomposed the equation into pure advection and pure diffusion parts, and solved the advection equation using the Holly-Preissmann method with cubic interpolating polynomial, and solved the diffusion equation using the Crank-Nicholson scheme. One-dimensional version of their method is used as a numerical method for the longitudinal dispersion equation of the stream water quality model CE-QUAL-RIV1 (Environmental Laboratory, 1990). The split-operator method yields very accurate simulations which are free from numerical diffusion or oscillations. However, treating advection and diffusion as independent processes is not physically justificable, and additional upstream boundary conditions are needed for the diffusion calculation. Toda and Holly (1987) developed a hybrid numerical method which treats advection and diffusion simultaneously. They used the cubic interpolating polynomial in the approximation of the time derivative, and a Crank-Nicholson type of approximation for the diffusion term. In this study a hybrid numerical method with the fifth-degree interpolating polynomial is introduced, which is extended to be applicable for Courant numbers greater than unity. The hybrid methods are applied, together with the split-operator methods to a longitudinal dispersion problem where exact solution exists, and the computational results are compared.

2. Description of the Hybrid Method

The equation for longitudinal dispersion in a one-dimensional prismatic channel can be represented by one of the following two forms :

$$\frac{\partial C}{\partial t}+U\frac{\partial C}{\partial x}=D\frac{\partial^2 C}{\partial x^2}, \text{ for all x and t} \tag{1}$$

or

$$\frac{dC}{dt}=D\frac{\partial^2 C}{\partial x^2}, \text{ along the characteristic line } \frac{dx}{dt}=U \tag{2}$$

in which C(x, t) is the concentration ; U and D are mean flow velocity and longitudinal dispersion coefficient, respectively, which are assumed to be constant; and x and t are space and time coordinates, respectively. Two-time-level Eulerian schemes approximate the partial derivatives in each term of Eq. (1), and the resulting difference equation consists of some of the discrete values for the fixed grid points (i−1,n), (i,n), (i+1,n), (i−1,n+1), (i,n+1), (i+1,n+1). On the other hand, the hybrid method takes finite difference form of Eq. (2) as follows : (see Fig. 1).

$$C_i^{n+1} = C_\xi^n + D\Delta t\left[(1-\theta)\left(\frac{\partial^2 C}{\partial x^2}\right)_\xi^n + \theta\left(\frac{\partial^2 C}{\partial x^2}\right)_i^{n+1}\right] \tag{3a}$$

$$= C_\xi^n + D\Delta t(1-\theta)Cxx_\xi^n + \frac{D\Delta t}{(\Delta x)^2}\theta\left(C_{i+1}^{n+1} - 2C_i^{n+1} + C_{i-1}^{n+1}\right) \tag{3b}$$

where ξ is the position at time level n of the characteristic line which passes through (i, n+1), and can be written as

$$\xi = i - \frac{U\Delta t}{\Delta x} \tag{4}$$

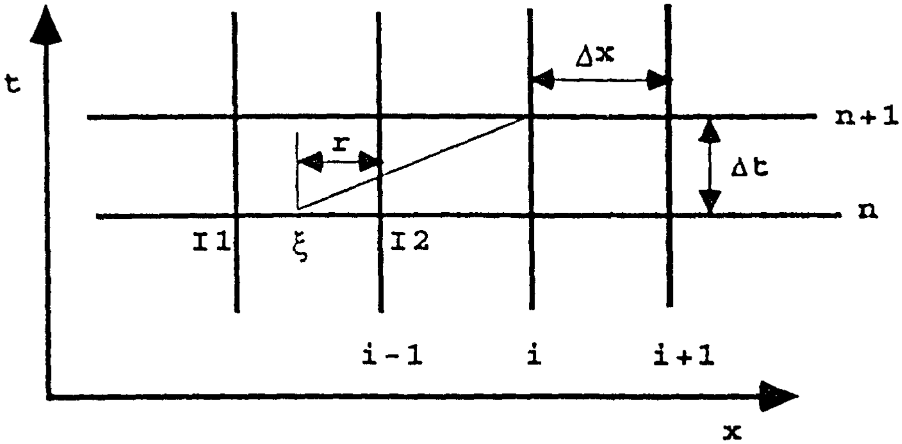

Fig. 1. Schematic Representation of the Numerical Scheme

Cxx represents the second-order partial derivative of C with respect to x, and the weighting factor θ, has a value between 0 and 1. Eq. (3b) is analogous to the difference equation for the generalized Crank-Nicholson scheme in the sense that the time derivative, dC/dt is approximated by a divided difference between time levels, n and n+1 and that the second-order spatial derivative is approximated by a weighted average of those for time levels, n and n+1. However, unlike the usual Crank-Nicholson scheme, it reflects the hyperbolicity of the equation by using the informations, C and Cxx, at (ξ, n) instead of those for (i,n). C_ξ^n in Eq. (3b) is given by the following interpolating polynomial (see Fig. 1)

$$C_\xi^n(r) = a_0 + a_1 r + a_2 r^2 + a_3 r^3 + a_4 r^4 + a_5 r^5 \tag{5}$$

$$r = I2 - \xi \quad (6)$$

From Eqs. (4) and (6) one can see that r is equal to the Courant number if i and I2 are identical, which implies that the Courant number is less than 1. If the Courant number is greater than 1, r is equal to the decimal part of the Courant number (see Fig. 1).

Coefficients of the interpolating polynomial can be obtained from the following six boundary conditions, two for each of C, Cx (first-order spatial derivative of C) and Cxx :

$C_\xi^n(0) = C_{I2}^n$, $C_\xi^n(1) = C_{I1}^n$, $Cx_\xi^n(0) = Cx_{I2}^n$,

$Cx_\xi^n(1) = Cx_{I1}^n$, $Cxx_\xi^n(0) = Cxx_{I2}^n$ and $Cxx_\xi^n(1) = Cxx_{I1}^n$.

The coefficients so obtained are

$$a_0 = C_{I2}^n \quad (7)$$

$$a_1 = -\Delta x\, Cx_{I2}^n \quad (8)$$

$$a_2 = \frac{1}{2}(\Delta x)^2\, Cxx_{I2}^n \quad (9)$$

$$a_3 = 10C_{I1}^n - 10C_{I2}^n + 4\Delta x Cx_{I1}^n + 6\Delta x\, Cx_{I2}^n + \frac{1}{2}(\Delta x)^2\, Cxx_{I1}^n - \frac{3}{2}(\Delta x)^2\, Cxx_{I2}^n \quad (10)$$

$$a_4 = -15C_{I1}^n + 15C_{I2}^n - 7\Delta x Cx_{I1}^n - 8\Delta x\, Cx_{I2}^n - (\Delta x)^2\, Cxx_{I1}^n + \frac{3}{2}(\Delta x)^2\, Cxx_{I2}^n \quad (11)$$

$$a_5 = 6C_{I1}^n - 6C_{I2}^n + 3\Delta x Cx_{I1}^n + 3\Delta x\, Cx_{I2}^n + \frac{1}{2}(\Delta x)^2\, Cxx_{I1}^n - \frac{1}{2}(\Delta x)^2\, Cxx_{I2}^n \quad (12)$$

Thus, the values of Cx and Cxx as well as C at (I1,n) and (I2,n) are required. Cx and Cxx at computational grid points can be obtained by solving the following longitudinal dispersion equations for Cx and Cxx which are derived, respectively, by taking the first-and the second-order spatial derivatives of Eq. (2).

$$\frac{dCx}{dt} = D\frac{\partial^2 Cx}{\partial x^2}, \text{ along the characteristic line } \frac{dx}{dt} = U \quad (13)$$

$$\frac{dCxx}{dt} = D\frac{\partial^2 Cxx}{\partial x^2}, \text{ along the characteristic line } \frac{dx}{dt} = U \quad (14)$$

These two equations must be solved at each time level together with Eq. (2).

Finite difference equations for Eqs. (13) and (14), similarly to that for Eq. (2), can be written as

$$Cx_i^{n+1} = Cx_\xi^n + D\Delta t(1-\theta)Cxxx_\xi^n + \frac{D\Delta t}{(\Delta x)^2}\theta\,(Cx_{i+1}^{n+1} - 2Cx_i^{n+1} + Cx_{i-1}^{n+1}) \quad (15)$$

$$Cxx_i^{n+1} = Cxx_\xi^n + D\Delta t(1-\theta)Cxxxx_\xi^n + \frac{D\Delta t}{(\Delta x)^2}\theta\,(Cxx_{i+1}^{n+1} - 2Cxx_i^{n+1} + Cxx_{i-1}^{n+1} \quad (16)$$

Cx_ξ^n, Cxx_ξ^n, $Cxxx_\xi^n$ and $Cxxxx_\xi^n$ in Eqs. (3b), (15) and (16) can be obtained from Eq. (5)

using the following relation,

$$\frac{\partial}{\partial x}=\frac{\partial}{\partial r}\frac{\partial r}{\partial x}=-\frac{1}{\Delta x}\frac{\partial}{\partial r} \tag{17}$$

and can be written in the following form :

$$\left(\frac{\partial^k C}{\partial x^k}\right)_\xi^n=\alpha_{1k}\, C_{I1}^n+\alpha_{2k}\, C_{I2}^n+\alpha_{3k}\, Cx_{I1}^n+\alpha_{4k}\, Cx_{I2}^n+\alpha_{5k}\, Cxx_{I1}^n+\alpha_{6k}\, Cxx_{I2}^n \tag{18}$$

where α_{ik}'s are tabulated as Table 1. If the Courant number is greater than 1, some characteristic lines passing through (i,n+1) cross the t-axis between time levels n and n+1 (see Fig. 1). In that case C_{I1}, C_{I2}, Cx_{I1}, Cx_{I2}, Cxx_{I1} and Cxx_{I2} are given by the upstream boundary conditions for C, Cx and Cxx.

Table 1. Coefficients for the Computation of C, Cx and Cxx at ξ

k	0	1	2	3	4
α_{1k}	$r^3(10-15+6r^2)$	$-30r^2(1-r)^2/\Delta x$	$60r(1-3r+2r^2)/(\Delta x)^2$	$-60(1-6r+6r^2)/(\Delta x)^3$	$360(2r-1)/(\Delta x)^4$
α_{2k}	$1-\alpha_{10}$	$1-\alpha_{11}$	$-\alpha_{13}$	$-\alpha_{13}$	$-\alpha_{14}$
α_{3k}	$r^3(1-r)(4-3r)\Delta x$	$-r^2(2-3r)(6-5r)$	$12r(1-r)(2-5r)/\Delta x$	$-12(2-14r+15r^2)/(\Delta x)^2$	$24(-7+15r)/(\Delta x)^3$
α_{4k}	$-r(1-r)^3(1+3r)\Delta x$	$(1-r)^2(1-3r)(1+5r)$	$12r(1-r)(3-5r)/\Delta x$	$12(3-16r+15r^2)/(\Delta x)^2$	$24(-8+15r)/(\Delta x)^3$
α_{5k}	$r^3(1-r)^2(\Delta x)/2$	$-r^2(1-r)(3-5r)\Delta x/2$	$r(3-12r+10r^2)$	$-3(1-8r+10r^2)/\Delta x$	$12(-2+5r)/(\Delta x)^2$
α_{6k}	$r^2(1-r)^3(\Delta x)/2$	$-r(1-r)^2(2-5r)\Delta x/2$	$(1-r)(1-8r+10r^2)$	$3(3-12r+10r^2)/\Delta x$	$12(3-5r)/(\Delta x)^2$

Eqs. (3b), (15) and (16) can be rewritten, respectively, as follows :

$$PC_{i-1}^{n+1}+(1-2P)C_i^{n+1}+PC_{i+1}^{n+1}=S_\xi \tag{19}$$

$$PCx_{i-1}^{n+1}+(1-2P)Cx_i^{n+1}+PCx_{i+1}^{n+1}=Sx_\xi \tag{20}$$

$$PCxx_{i-1}^{n+1}+(1-2P)Cxx_i^{n+1}+PCxx_{i+1}^{n+1}=Sxx_\xi \tag{21}$$

where

$$P=-\frac{D\Delta t}{(\Delta x)^2}\theta \tag{22}$$

$$S_\xi=C_\xi^n+D\Delta t(1-\theta)Cxx_\xi^n \tag{23}$$

$$Sx_\xi=Cx_\xi^n+D\Delta t(1-\theta)Cxxx_\xi^n \tag{24}$$

$$Sxx_\xi=Cxx_\xi^n+D\Delta t(1-\theta)Cxxxx_\xi^n \tag{25}$$

Given appropriate upstream and downstream boundary conditions, Eqs. (19), (20) and (21), respectively, constitute systems of linear equations with three unknowns for time level n+1. Since these systems have a tridiagonal structure, they can be solved by the Thomas algorithm (Carnahan et al., 1969), which requires the least amount of calculations.

Stability condition for the hybrid method is too complex to express as an explicit functional relationship as those for Eulerian schemes (Kang and Lee, 1987; Anderson et al., 1984), and it is left for future study. Whether the method is stable for given values of θ, Courant number and Diffusion number($=D\Delta t/(\Delta x)^2$) may be determined by the von Neumann matrix stability analysis. Stability analysis for the hybrid method using cubic interpolating polynomial is given by Toda and Holly (1987).

3. Model Application

The numerical model was tested by computing longitudinal dispersion of an instantaneously loaded Gaussian contaminant distribution, for which an analytic solution exists. A number of error measures were computed to analyze the test results. The computational results were compared with the analytic solution and with those from the hybrid method using cubic interpolating polynomial (Toda and Holly, 1987) and with those by split-operator methods using Holly-Preissmann scheme for pure advection and Crank-Nicholson scheme for pure diffusion (Holly and Preissmann, 1977; Environmental Laboratory, 1990; Jun and Lee, 1994).

3.1 Initial and Boundary Conditions

The analytic solution to Eq. (1) for an instantaneous plane source M (mass per unit area) released at time, t=0 at the point, x=0 is given by (Fischer et al., 1979)

$$C(x,\ t)=\frac{M}{\sqrt{4\pi Dt}}\ \exp\left[-\frac{(x-Ut)^2}{4Dt}\right] \tag{26}$$

The spatial distribution at t=3200 s, with $M=3000\ kg/m^2$ and $U=0.5\ m/s$ was taken as the initial condition. Two different values for the longitudinal dispersion coefficient, $D=2$ and $10\ m^2/s$, were tried. Longitudinal dispersion of the Gaussian distribution, C(x,3200) from Eq. (26), was simulated for 9600 seconds. Exact solution at the end of the computation is given by Eq. (26) with t=12800. Exact solutions corresponding to each value of D are shown in Fig. 2 together with the initial conditions. Initial conditions for Cx and Cxx are given by the first-and the second-order spatial derivatives, respectively, of Eq. (26) with t=0.

Concentration at the upstream end, C_0, and its first-and second-order derivatives, Cx_0 and Cxx_0, were taken as zero. Consequently, the upstream boundary conditions for C, Cx and Cxx are, respectively, given by Eqs. (19), (20) and (21) with i=1 and with C_0, Cx_0 and Cxx_0 equal to zero. Cx_I and Cxx_I (Cx and Cxx at the downstream end) were also taken as zero; thus, the downstream boundary conditions for Cx and Cxx are given by Eqs. (20) and (21), respectively, with $i=I-1$ and third terms on the left hand side equal to zero. Zero concentration was imposed as downstream boundary condition for C, which can be expressed as

$$PC_{I-1}^{n+1}+(1-P)C_{I}^{n+1}=S_{e} \tag{27}$$

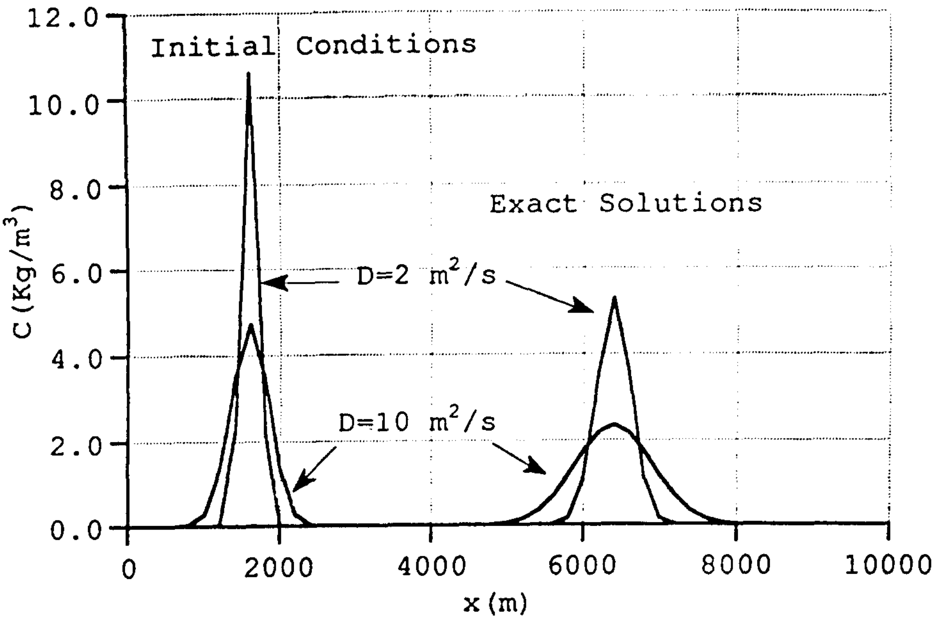

Fig. 2 Initial Conditions and Exact Conditions

3.2 Computational Results and Analysis

Fig. 3 shows comparisons with the exact solution of the concentration distributions for various values of θ with D=2 m²/s. Time and space increments, t and x, and thus the Courant number, $U\Delta t/\Delta x$ were set to 200 s, 200 m, and 0.5, respectively. It is seen that computational results for various values of θ are almost identical to the exact solution except near the position of peak concentration. Concentration distributions were simulated by the present method and by the hybrid method using cubic interpolating polynomial for Courant numbers 0.25, 0.50, 0.75 and 1.50. Δx was set to constant 200 m and Δt was varied as 100, 200, 300 and 600 s to produce the above Courant numbers. The following error measures, proposed by Noye (1987), were used to analyze the accuracy of each method.

$$E_1=\sum_{i=1}^{I}|C_i-CE_i|/\sum_{i=1}^{I}CE_i \tag{28}$$

$$E_2=(C_{max}-CE_{max})/CE_{max} \tag{29}$$

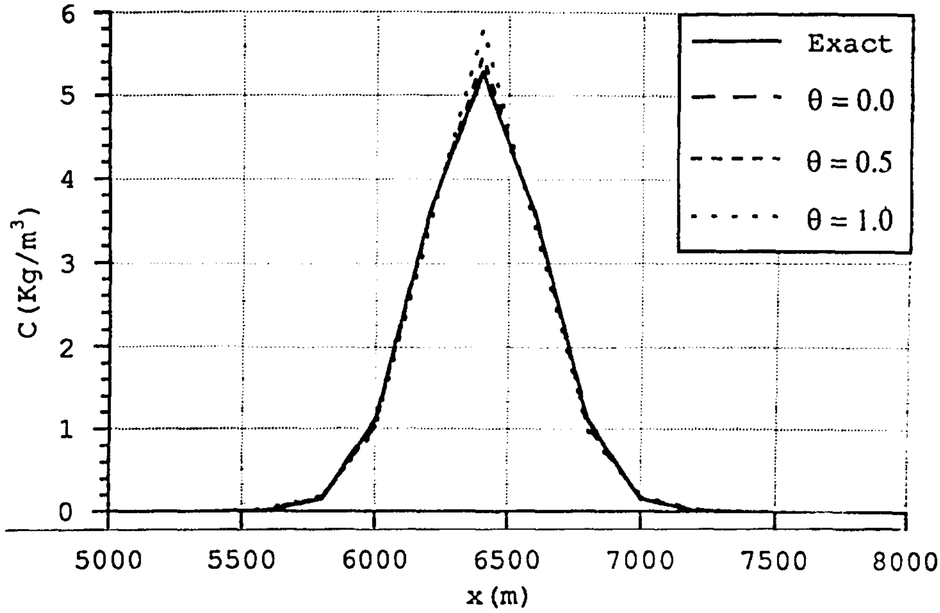

Fig. 3 Computational Results for Various Weighting Factors ($D=2m^2/s$)

$$E_3=\text{Min}(C_i)/CE_{max} \tag{30}$$

$$E_4=(X_p-XE_p)/\Delta x \tag{31}$$

where C and CE represent the concentration simulated by the model and the exact solution, respectively. X_p and XE_p are positions of peak concentration simulated by the model and from the exact solution, respectively. Among the dimensionless error measures defined above, E_1 represents overall accuracy, which takes the value $E_1=0$ if C is exact. Negative values of E_2 and E_3 indicate numerical diffusion and oscillations, respectively, whose absolute values become larger as they become more severe. E_4 is the peak lead expressed in terms of grid spacings. The results of accuracy analysis for various values of θ and Courant numbers are summarized in Table 2. In the following discussions HYBRID(3) and HYBRID(5) represent hybrid methods using interpolating polynomials of degree 3 and 5, respectively. It is seen that HYBRID(5) is free from numerical oscillations regardless of the Courant number while HYBRID(3) gives slight oscillations. Positions of peak concentration simulated by both methods are identical to the exact solution. Negative values of E_2 in case of HYBRID(3) indicate numerical diffusion. On the other hand, HYBRID(5) results in positive values of E_2, except for the case $\theta=0$, which implies overestimation of the peak concentration. E_2 for HYBRID(5) is more sensitive to the weighting factor θ than that for HYBRID(3). In case of HYBRID(3) E_1 decreases, or overall accuracy improves with increasing θ while the opposite tendency is observed for HYBRID(5). These tendencies are common to all cases of Courant number. Also

Table 2. Analysis of Results for Various Courant Numbers and Weighting Factors (D=2 m^2/s)

(a) Hybrid Method with Fifth-Degree Interpolating Polynomial

Courant Number	θ	E_1	E_2	E_3	E_4
0.25	0.0	0.009	-0.007	0	0
	0.25	0.009	0.009	0	0
	0.5	0.024	0.027	0	0
	0.75	0.045	0.049	0	0
	1.0	0.068	0.076	0	0
0.50	0.0	0.007	-0.006	0	0
	0.25	0.010	0.012	0	0
	0.5	0.030	0.033	0	0
	0.75	0.053	0.060	0	0
	1.0	0.083	0.097	0	0
0.75	0.0	0.008	-0.007	0	0
	0.25	0.010	0.012	0	0
	0.5	0.031	0.035	0	0
	0.75	0.055	0.063	0	0
	1.0	0.085	0.101	0	0
1.50	0.0	0.013	-0.012	0	0
	0.25	0.007	0.010	0	0
	0.5	0.031	0.036	0	0
	0.75	0.060	0.070	0	0
	1.0	0.101	0.121	0	0

(b) Hybrid method with Cubic Interpolating Polynomial

Courant Number	θ	E_1	E_2	E_3	E_4
0.25	0.0	0.152	-0.138	-0.022	0
	0.25	0.149	-0.135	-0.022	0
	0.5	0.146	-0.132	-0.022	0
	0.75	0.143	-0.129	-0.021	0
	1.0	0.141	-0.126	-0.021	0
0.50	0.0	0.094	-0.095	-0.012	0
	0.25	0.089	-0.090	-0.011	0
	0.5	0.084	-0.085	-0.010	0
	0.75	0.079	-0.080	-0.009	0
	1.0	0.073	-0.075	-0.008	0
0.75	0.0	0.056	-0.055	-0.005	0
	0.25	0.049	-0.047	-0.004	0
	0.5	0.041	-0.039	-0.003	0
	0.75	0.035	-0.031	-0.002	0
	1.0	0.031	-0.023	-0.001	0

observed is that overall accuracy of HYBRID(3) improves with increasing Courant number, or time step Δt. However, HYBRID(5) yields more accurate result for smaller Courant number. Sensitivity of E_1 to the Courant number decreases as the weighting factor θ decreases. For θ less than 0.5, HYBRID(5) gives smaller E_1, E_2, and E_3 errors, for all Courant numbers, than HYBRID(3).

Table 3 and Fig. 4 represent comparisons, respectively, of the results of accuracy analysis and of the concentration distributions simulated with Courant number 0.5 and $\theta = 0.5$. In addition to the two hybrid methods two split-operator methods were used. The split-operator methods decompose the equation into pure advection and pure diffusion parts, using the Holly-Preissmann method for advection calculation and the Crank-Nicholson scheme for diffusion calculation. SPLIT(3) and SPLIT(5) represent the split-operator methods which use the interpolating polynomials of degree 3 and 5, respectively, for the advection calculation. It is seen that if the interpolating polynomial of degree 3 is used, both the hybrid and the split-operator methods result in slight numerical diffusion and oscillations. On the other hand, SPLIT(5) and HYBRID(5), which use the interpolating polynomial of degree 5, give no numerical oscillations at all, but slightly overestimate the peak concentration. One can also see that using higher degree interpolating polynomial gives more accurate results in case of the hybrid method while it does not in case of the split-operator method. From Tables 2 and 3 it is seen that HYBRID(5) with $\theta = 0.5$ shows the best performance in minimizing the error measures.

Table 3. Analysis of Results by Various Characteristics-Based Methods ($D = 2 m^2/s$)

Method	Courant Number	E_1	E_2	E_3	E_4
SPLIT(3)	0.25	0.141	-0.127	-0.021	0
	0.50	0.075	-0.076	-0.008	0
	0.75	0.033	-0.026	-0.001	0
SPLIT(5)	0.25	0.066	0.074	-0.000	0
	0.50	0.079	0.093	0	0
	0.75	0.080	0.094	0	0
HYBRID(3)	0.25	0.146	-0.132	-0.022	0
	0.50	0.084	-0.085	-0.010	0
	0.75	0.041	-0.039	-0.003	0
HYBRID(5)	0.25	0.024	0.027	0	0
	0.50	0.030	0.033	0	0
	0.75	0.031	0.035	0	0

Results of the accuracy analysis for the case of $D = 10\ m^2/s$ are summarized in Table 4, and Fig. 5 is a comparison of concentration distributions simulated by various methods. For the Courant number of 0.75 and $\theta = 0$, HYBRID(5) resulted in numerical instability. It is seen that computational results by each method show much better accuracy than those for $D = 2\ m^2/s$. This is due to the reduction of the relative significance of the advection term compared to the diffusion term; in other words, most of the numerical errors come from the approximation of the advection term. HYBRID

(5) gives more accurate result for smaller value of θ and overestimates the peak concentration as θ becomes larger, which are also the cases with D=2 m²/s.

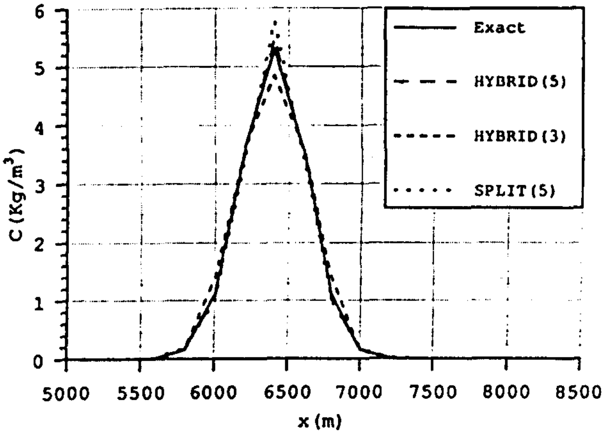

Fig. 4 Comparison of Results by Various Methods (D=2m²/s)

Table 4. Analysis of Results by Various Characteristics–Based Methods (D=10m²/s)

Method	Courant Number		E_1	E_2	E_3	E_4
SPLIT(3)	0.25		0.0018	0.0003	-0.0000	0
	0.50		0.0053	0.0058	0	0
	0.75		0.0092	0.0102	0	0
SPLIT(5)	0.25		0.0138	0.0155	0	0
	0.50		0.0139	0.0156	0	0
	0.75		0.0138	0.0155	0	0
HYBRID(3)	0.25	θ=0.0	0.0094	-0.0099	-0.0000	0
		θ=0.5	0.0034	-0.0036	-0.0000	0
		θ=1.0	0.0027	0.0022	0	0
	0.50	θ=0.0	0.0055	-0.0059	0	0
		θ=0.5	0.0017	-0.0018	0	0
		θ=1.0	0.0009	-0.0100	0	0
	0.75	θ=0.0	0.0175	-0.0161	-0.0005	0
		θ=0.5	0.0044	0.0046	0	0
		θ=1.0	0.0149	0.167	0	0
HYBRID(5)	0.25	θ=0.0	0.0021	-0.0022	0	0
		θ=0.5	0.0066	0.0073	0	0
		θ=1.0	0.0158	0.0178	0	0
	0.50	θ=0.0	0.0040	-0.0044	0	0
		θ=0.5	0.0066	0.0072	0	0
		θ=1.0	0.0179	0.0202	0	0
	0.75	θ=0.0	unstable	unstable		
		θ=0.5	0.0064	0.0071	0	0
		θ=1.0	0.0198	0.0225	0	0

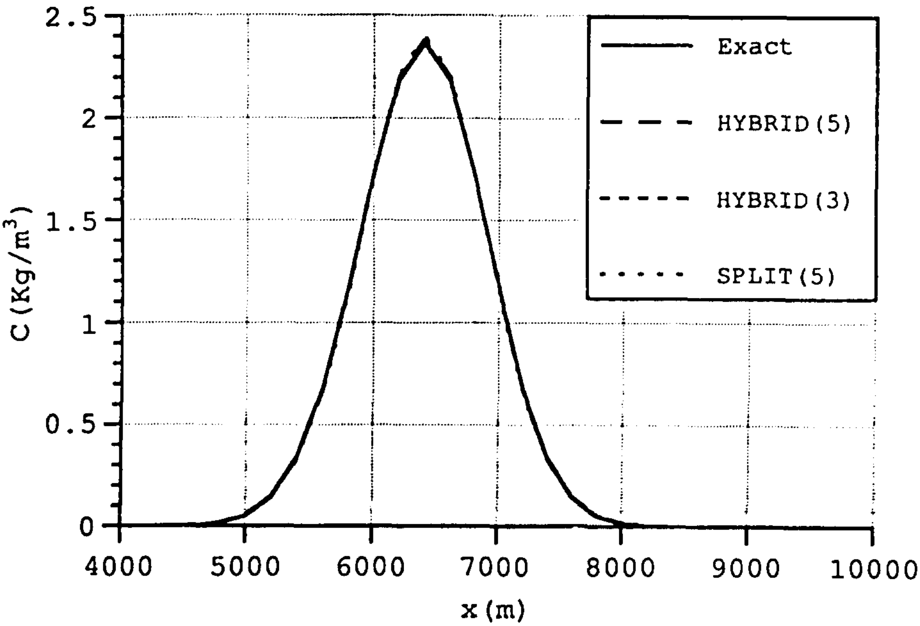

Fig. 5 Comparison of Results by Various Methods ($D=10m^2/s$)

4. Conclusions

A hybrid numerical method for the longitudinal dispersion equation based on the Holly-Preissmann scheme with fifth-degree Hermite interpolating polynomial and the generalized Crank-Nicholson scheme was tested by computing longitudinal dispersion of an instataneously loaded Gaussian contaminant distribution, for which an analytic solution exists. As a result the followings were found.

The method was free from wiggles while the hybrid method with cubic interpolating polynomial yielded slight oscillations, and exactly reproduced the location of the peak concentration. Computational accuracy increased for smaller Courant number, but the sensitivity to the Courant number was very low, especially when the value of the weighting factor, θ was small. The model resulted in no numerical diffusion, but overesimated the peak concentration as θ becomes large. Overall accuracy increased with decreasing θ. From comparisons with the hybrid method using cubic interpolating polynomial and with split-operator methods, the present method yielded more accurate result as the advection becomes more dominant.

References

1. Abbott, M.B. and Basco, D.R. (1989). *Computational Fluid Dynamics : An Introduction for Engineers*, Longman Scientific & Technical, London, Chapters 4 and 5.

2. Anderson, D.A., Tannehill, J.C., and Pletcher, R.H. (1984). *Computational Fluid Mechanics and Heat Transfer*, McGraw-Hill, New York, Chapter 4.
3. Bresler, E. (1973). "Simultaneous transport of solutes and water under transient unsaturated flow conditions", *WRR*, Vol. 9, No. 4, pp. 975-986.
4. Carnahan, B., Luther, H.A., and Wilkes, J.O. (1969). *Applied Numerical Methods*, John Wiley & Sons, New York, pp. 441-442.
5. Chaudhari, N.M. (1971). "An improved numerical technique for solving multidimensional miscible displacement equations", *J. Soc. Petroleum Engrs.*, Vol. 11, Sept., pp. 277-284.
6. Environmental Laboratory (1990). *CE-QUAL-RIV1 : A Dynamic, One-Dimensional ·(Longitudinal) Water Quality Model for Streams*, U.S. Army Corps of Engineers, Waterways Experiment Station, Vicksburg, Mississsippi, pp. 37-46.
7. Fischer, H.B., List, E.J., Koh, R.C.Y., Imberger, J., and Brooks, N.H. (1979). *Mixing in Inland and Coastal Waters*, Academic Press, Orlando, Chapter 2.
8. Holly, F.M. and Preissmann, A. (1977). "Accurate calculation of transport in two dimensions", *J. Hyd. Div.*, ASCE, Vol. 103, No. 11, pp. 1259-1277.
9. Holly, F.M. and Usseglio-Polatera, J.M. (1984). "Pollutant dispersion in tidal flow", *J. Hyd. Engrg.*, ASCE, Vol. 110, No. 7, pp. 905-926.
10. Jun, K.S. and Lee, K.S. (1994). "Eulerian-Lagrangian split-operator method for the longitudinal dispersion equation", *Proc. Korean Society of Civil Engineers*, Vol. 14, No. 1, pp. 131-141.
11. Kang, J.W. and Lee, K.S. (1987). "Characteristics of the finite difference approximations for the convective dispersion model", *Proc. Korean Society of Civil Engineers*, Vol. 7, No. 4, pp. 147-157.
12. Leonard, B.P. (1979). "A stable accurate convective modelling procedure based on quadratic upstream interpolation", *Computer Methods in Applied Mechanics and Engineering*, Vol. 19, pp. 59-98.
13. Noye, J. (1987). "Numerical methods for solving the transport equation", in *Numerical Modelling: Applications to Marine Systems*, ed. J. Noye, Elsevier, Amsterdam, pp. 195-229.
14. Toda, K. and Holly, F.M. (1987). "Hybrid numerical method for linear advection-diffusion", *Microsoftware for Engineers*, Vol. 3, No. 4, pp. 199-205.
15. Yoon, T.H. (1979). "Longitudinal dispersion of pollutants in streams of irregular cross section", *J. Korean Society of Civil Engineers*, Vol. 27, No 3, pp. 83-87.